Malaysian Journal of Chemistry, 2022, Vol. 24(2), 59-69
(Special Issue: *2nd IKM Pahang Branch Symposium 2022 – Sustainability & Diversity Through Chemistry*)

Photocatalytic Synthesis of Propanol from Glycerol with Fluorine-doped Tin Oxide (FTO)

Sadina Shazwani Mastika[1], Aishah Hanis Abdul Majid[1], Norazzizi Nordin[2] and Wan Zurina Samad[1]*

[1]Department of Chemistry, Kulliyyah of Science, International Islamic University Malaysia, IIUM Kuantan Campus, Jalan Sultan Ahmad Shah, Bandar Indera Mahkota, 25200 Kuantan, Pahang Darul Makmur, Malaysia

[2]School of Chemical Sciences, Universiti Sains Malaysia, 11800 Gelugor, Pulau Pinang, Malaysia

*Corresponding author (e-mail: wzurina@iium.edu.my)

Glycerol is the major by-product of biodiesel produced by the transesterification process. It is abundantly produced, and thus has a low market price although it requires high-cost purification processes and can cause environmental problems. Because of this, efficient utilization of glycerol is necessary to avoid oversupply. In this preliminary study, the photocatalytic conversion of glycerol to propanol using fluorine-doped tin oxide (FTO) is proposed for the first time. This method produces propanol with high selectivity under optimal reaction conditions. For the identification of the conversion product, the surface morphology, composition, reaction yield, and physicochemical state of the prepared photocatalyst were comprehensively characterized by scanning electron microscopy (SEM), Energy Dispersive X-ray spectroscopy (EDX), X-ray diffraction analysis (XRD), X-Ray Photoelectron Spectroscopy (XPS) and high-performance liquid chromatography (HPLC). An optimum glycerol conversion of 86 % and a high propanol selectivity of 100 % was achieved under 80 W of UV light and 90 minutes of reaction time using 10 wt% glycerol solution. The FTO photocatalyst proved very dynamic as various products may be formed under different reaction conditions by optimizing parameters such as reaction time, light, and glycerol concentration.

Key words: Photocatalyst; fluorine-doped tin oxide (FTO); free radical; glycerol conversion; propanol

Received: December 2021; Accepted: February 2022

The abundance of glycerol production, specifically as a side product of palm oil transesterification, has led to a decrease in its commercial price in the world market [1]. Additionally, the disposal of crude glycerol can be costly, detrimental to the environment and wasteful. Hence, it is crucial to ensure efficient utilization of this substance. Consequently, an oversupply of glycerol may be overcome by maximizing its benefits [2] toward value-added products useful in daily life.

Glycerol can be converted into promising commodity chemicals and fuels through chemically selective catalysis such as selective oxidation, selective hydrogenolysis, catalytic dehydration, pyrolysis and gasification, selective glycerol transesterification and esterification, selective etherification and carboxylation and other processes [3]. Among the products of those processes are acrolein, acrylic acid, hydroxyacetone, allyl alcohol, epichlorohydrin, lactic acid, 1,2-propanediol (1,2-PDO), 1,3-propanediol (1,3-PDO), propanol (PrOH) and very recently ethanol (EtOH) [4]. These products benefit industrial commercialization as they have high profitability in the world market. Propanol, that has various applications such as a solvent for organic intermediates, is one of the beneficial products resulting from glycerol conversion in this study.

Previously, many studies have been done on the conversion of glycerol to propanol through hydrogenolysis of glycerol in a fixed-bed reactor, with the addition of hydrogen. This method seems to have low selectivity for propanol, which is mostly considered as a side product of glycerol conversion in the range of 80 % to 100 % [5-7]. Furthermore, this process takes a long time, leading to high energy consumption, and depends greatly on a bifunctional catalyst. Crude glycerol contains matter organic non-glycerol (MONG), which makes the catalyst surface dirty, blocks active sites and can act as coke precursors. Hence, a bifunctional catalyst is used to overcome this problem. However, the catalyst is expensive, and in some cases, favours undesirable C-C bond cleavage reactions [8]. Plus, most glycerol conversion reactions need higher energy with high reaction temperatures, and are time-consuming as they require a bioreactor as the medium for conversion. Most conversion activities in a bioreactor require high temperatures in the range of 200 °C - 350 °C over 3 to 24 hours [8].

†Paper presented at the 2nd IKM Pahang Branch Symposium 2022 – Sustainability & Diversity Through Chemistry

Table 1. Summary of experimental conditions and efficiency of glycerol photoconversion methods from previous studies

Photocatalyst type	Glycerol content (wt%)	Irradiation source	Volume of irradiated solution (ml)	Selectivity of product	Glycerol conversion (%)	Reference
Pt/TiO_2	9.0	Xe arc lamp, 225 W	100 ml	10.0 mmol· h^{-1} · g_{cat}^{-1} of H_2 after 3h	5.0	[12]
Pt/ TiO_2	4.4	Xe arc lamp, 225 W	15 ml	15.6 mmol· h^{-1} · g_{cat}^{-1} of H_2 after 3h	14.4	[12]
α-Bi_2O_3	2.2	UV high pressure mercury lamp, 20 W	100 ml	25 % of Glyoxylic acid after 4 h	80.0	[13]
Cel-TiO_2	0.5	Metal halide lamp, 400 W	200 ml	50% of Folic acid after 8 h	70.0	[9]

The drawbacks of the conventional conversion process may be reduced by using a photocatalysis method [9]. Photocatalysis has been developed as an artificial photosynthesis technique that uses green, sustainable chemistry to solve energy and environmental issues [10]. Photocatalytic processing is a green, versatile, and powerful toolbox for synthesising many important chemicals under ambient conditions without applying additional redox reagents. It does not consume much energy, has a shorter reaction time, and uses fewer reagents [11]. It also has the advantage of energy-saving by utilizing solar power with suitable photocatalysts. Indeed, many studies have proved successful at converting glycerol into value-added chemicals using photocatalysis with various catalysts and parameters. As summarized in Table 1, different catalysts were used for glycerol conversion, and product selectivity was quite high. Therefore, this is a promising method as it requires little energy and does not pollute the environment.

Photocatalysis of glycerol into propanol may become profitable if new and more efficient photocatalysts are introduced. Conversion of glycerol would be improved by the presence of both basic and acid sites; thus, it is clear that a fluorine-doped tin oxide (FTO) catalyst with amphoteric characteristics [14] would boost the reaction and produce promising results. FTO is commonly utilised as a transparent conducting oxide for semiconductors because it has a good band gap (2.6–3.6 eV) compared to indium tin oxide (ITO) and antimony tin oxide (ATO) [14-15,17-21]. FTO is classified as an n-type semiconductor with a cloud of delocalized electrons that can act as an electron donor. The electrons tend to be located near the conduction band, and thus, may be involved in redox reactions, such as in the conversion process of the reactant [17-21]. FTO also tends to have better physical and chemical properties than ITO and ATO, giving it the potential to be developed as a heterogeneous catalyst or photocatalyst in solar cells and gas sensors [15].

FTO also has a very good thermal and chemical stability which does not affect its catalytic activity in high-temperature reactions [17]. FTO was analysed using thermogravimetric analysis (TGA), and found to be thermally stable with no degradation curve until 430 °C and it did not show a specific degradation isotherm up to 1200 °C [18]. Due to these factors, FTO has become a significant photocatalyst to promote glycerol conversion and propanol selectivity. The use of FTO as an unsupported catalyst that has no additional metal reduces the utilization of metals in catalytic activity, promoting green catalytic conversion.

With its unique characteristics, FTO is currently widely used as a heterogeneous catalyst, either alone or as a support for a metal catalyst. For example, Ru/FTO was found very efficient for glycerol hydrogenolysis as it could enhance glycerol conversion (100%) and had a highest selectivity for 1,2-propanediol (94%) in a closed system reactor [14]. The use of FTO alone as a catalyst to produce high glycerol conversion (80%) and methanol selectivity (100%) has also been reported using a sub-critical water method [18]. These previous studies showed that FTO was capable of glycerol degradation. However, studies on the photocatalytic conversion of glycerol to propanol are still limited. This preliminary study was conducted to assess the competitiveness of FTO against existing methods and catalysts used for photocatalytic degradation of glycerol. This study also aimed to widen the application of FTO as a new photocatalyst to

successfully produce propanol from glycerol, as FTO has never been used in photocatalytic conversion. With the high demand for propanol in industry, this effort may help in maximizing the use of glycerol as a by-product of biofuel manufacturing.

MATERIALS AND METHODS

Materials

Tin (IV) chloride pentahydrate ($SnCl_4.5H_2O$, >98% purity), ammonium fluoride (NH_4F, >95%), ethylene glycol (>95%), ammonium hydroxide (NH_4OH, > 95%) and deionized water were used to prepare FTO. Glycerol (99.9%) and deionized water were used in the conversion reaction. Methanol, propanol, ethanol and isopropanol of 99.9% (HPLC Grade) purity were used in the preparation of High-Performance Liquid Chromatography (HPLC) standards. All chemicals were used with no further purification.

Catalyst Preparation

Approx. 10.0 g of $SnCl_4.5H_2O$ was dissolved in 70 ml deionized water in a sealed conical flask which was continuously stirred and heated for 30 minutes until all the tin (IV) chloride pentahydrate dissolved. Next, 30 ml of ethylene glycol was added into the flask while heating and stirring continued. The resulting slightly turbid solution was labelled as mixture A. Meanwhile, mixture B was prepared for fluorine sources. 2.0 g of NH_4F, which provided the fluorine element as a doping agent, were dissolved in 5 ml deionized water in a sealed container. After 30 minutes, mixture B was added to mixture A while maintaining stirring and heating for 1 hour to ensure complete mixing.

The mixture was left to cool for 30 minutes. Then NH_4OH was added dropwise until the desired pH was achieved (pH 9–10) and a cloudy precipitate appeared. The mixture was heated and stirred at 60 °C for another 4 hours to ensure complete mixing. The precipitate was separated by filtration and rinsed with deionized water repeatedly to remove any impurities. The precipitate was then dried in an oven at 110 °C. The dried catalyst was grounded to a fine uniform powder before being calcined in a furnace at 400 °C for 2 hours.

Catalyst Characterization

Surface morphology, particle size and elemental studies were conducted on the catalyst using a scanning electron microscope equipped with an electron dispersive x-ray analyser (SEM-EDX: SU6600, Hitachi High Technologies Corp). All calcined FTO catalysts were coated with gold to avoid a charging effect during the imaging process. Next, X-ray photoelectron spectroscopy (XPS: JPS-9030, JEOL) was also performed to support the elemental analysis of the FTO catalyst. X-ray diffraction (XRD: RINT 2000 V) analyses were also conducted (Cu radiation $\lambda = 1.5406$ Å, $2\theta = 20$ to 80^o) to characterize the crystallinity and phase properties of the FTO catalyst.

Catalytic Activity

In the glycerol conversion experiment, 10 wt% solutions of glycerol feedstock were prepared by diluting 2 ml of glycerol in 20 ml deionized water. Then, 1.0 g of FTO catalyst powder was loaded into the glycerol feedstock solution. The mixture was continuously stirred to obtain complete adsorption of glycerol on the FTO surface. The mixture was irradiated with 20 watts of UV light. This experiment was conducted in a box to ensure complete darkness, using a 50 ml beaker equipped with a hot plate, thermometer, magnetic stirrer, and UV lamp, as illustrated in Figure 1. This experiment was repeated using different reaction parameters, as given in Table 2.

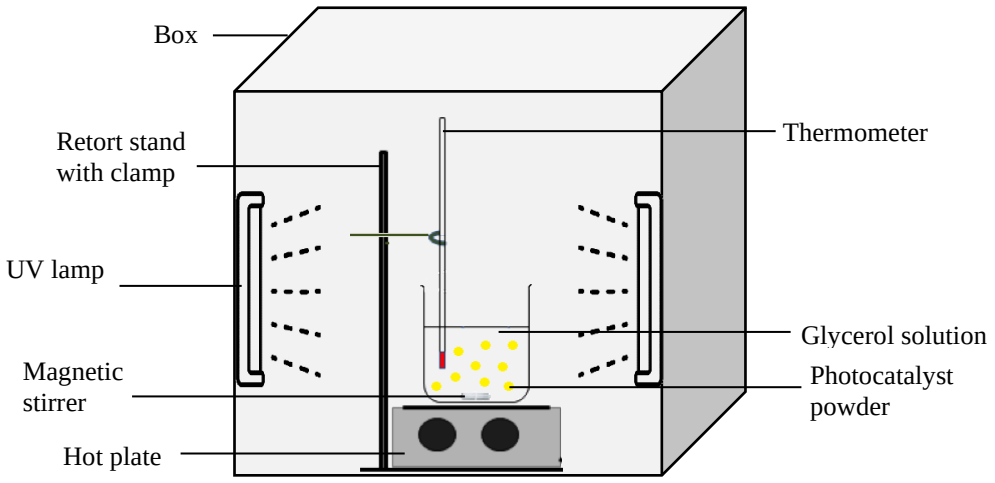

Figure 1. Photocatalysis set-up for conversion of glycerol, using UV light irradiation inside a sealed box.

Table 2. Reaction parameters for photocatalytic conversion of glycerol

Reaction parameter	Parameter value
Light wattage	20 W, 40 W, 60 W, 80 W
Reaction time	30 min, 60 min, 90 min
Glycerol concentration	10 wt%, 15 wt%, 20 wt%

Reaction Parameters

In these preliminary studies, three parameters were involved: light wattage, reaction time, and glycerol concentration. Table 2 shows the details of each parameter used during photocatalysis.

The first reaction was conducted by varying the light wattage and reaction time with 1.0 g FTO catalyst and 10 wt% glycerol. Based on the results obtained, the reaction with 80 W of light in 90 minutes had the most favourable result. Therefore, the 80 W and 90-minute reaction was optimized by varying glycerol concentrations to analyse which parameters affected photocatalytic activity.

After every reaction, product separation was done prior to analysis. The conversion product was left at room temperature before separation to ensure that the catalyst had completely precipitated at the bottom of the beaker. The separation of product and catalyst was done using filter paper and a filter funnel. The catalyst was collected using a Buchner funnel and filter paper. First, the used catalyst was rinsed twice with deionized water and once with methanol. Next, the used catalyst was dried in an oven at 110 °C to remove solvents and impurities. The dried, used catalyst was then weighed and compared with its original weight.

Product Characterization

The product was identified by chromatography using a Photodiode-Array Detection detector (HPLC-PDA, PerkinElmer). A reverse phase C18 column (Hypersil 5u ODS 120A, 150 x 4.60 mm, flow rate 0.6 ml/min) was used. The mobile phase was water and acetonitrile (ACN) with a ratio of 90:10, respectively. Analysis time was set at 15 minutes for each sample and the maximum oven temperature was 46.7 °C. Four standards were prepared which contained glycerol as the starting material and expected products such as ethanol, propanol, and methanol. The standard solutions were prepared by weighing a certain amount of each component into a beaker and then adding deionized water until the total weight was 10.0 g.

All standards and samples were filtered using a syringe filter (13 mm x 0.45 μm) before being transferred to a 1.5 ml vial. The samples were injected into the column using an autosampler. The standards were used as references for the samples based on the retention time. The peak areas of the standards were used to calculate the concentrations of the compounds based on the calibration curves. A graph of peak area vs concentration was plotted using Excel and a best fit straight line was plotted on the graph. The values of concentration, conversion, selectivity, and yield of components were obtained using equations 1 to 4.

Concentration (ppm), $x = \frac{y - c}{m}$, where y is peak area, c is y-intercept and m is the slope of the graph (Eqn 1)

$$\text{Conversion (\%)} = \frac{[\text{Glycerol}]_{\text{initial}} - [\text{Glycerol}]_{\text{final}}}{[\text{Glycerol}]_{\text{initial}}} \times 100\% \quad \text{(Eqn 2)}$$

$$\text{Selectivity (\%)} = \frac{\text{Peak area of product formed}}{\text{Peak area of total product obtained}} \times 100\% \quad \text{(Eqn 3)}$$

Yield (%) = Conversion x Selectivity x 100% (Eqn 4)

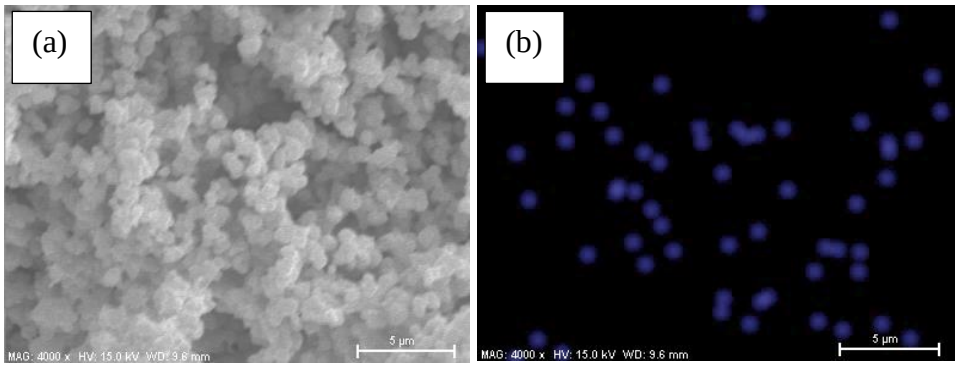

Figure 2. SEM images of (a) calcined FTO catalyst, and (b) mapping analysis of fluorine element by EDX

RESULTS AND DISCUSSION

Catalyst Characterization

The surface morphology of the FTO catalyst samples was studied using SEM, while mapping analysis was conducted using an EDX analyser. Figure 2 illustrates the SEM morphology image, and the fluorine cluster elemental mapping, respectively. It was observed that the FTO catalyst (Fig 2a) possessed a cassiterite structure represented by tetragonal rutile shapes [18-20]. Meanwhile, the particle size was in the range of 20 to 80 nm with a uniform distribution. Compared with a previous study [15], the FTO catalyst synthesized with this improved method using deionized water was seen to have an irregular shape and tended to agglomerate. This may be due to the solvent-solvent interaction whereby hydrogen bonding using water rather than alcohol occurred, causing a slowdown of drying, agglomeration, and a bigger particle size [(16)].

To ensure the existence of fluorine clusters in the FTO catalyst, mapping analysis was conducted. Figure (2b) shows that fluorine clusters were present and well distributed homogeneously on the FTO catalyst. The presence of all FTO catalyst elements was also confirmed with the EDX and XPS analyses. A summary of the chemical composition is presented in Table 3.

As displayed in Table 3, the major elements of the FTO catalyst, which comprised tin (Sn), oxygen (O), and fluorine (F), were successfully recorded. The calcined tin oxide sample (SnO_2) was taken as a standard for comparison with the FTO catalyst due to the similarity in their parent compounds. Significant analyses successfully proved the differences between SnO_2 and FTO in terms of the fluorine cluster footprint in the sample. Both EDX and XPS detected the presence of fluorine, thus suggesting that the fluorine cluster was successfully intercalated in the FTO catalyst molecule [15-18]. XPS composition analysis (the wide and narrow scan spectra are not included) was used confirm the existence of fluorine clusters and the chemical state of the element.

From XPS composition analysis, a significant peak detected with chemical bonding at 687.3 eV was attributed to the F 1s signal and it was assigned as the bonding of F-Sn. Considering the low intensity of the F 1s peak, it can be concluded that the fluorine clusters do appear in the FTO molecules in the form of physical and chemical bonding. Some fluorine clusters were proposed to behave as free electrons (fluoride ions) and were closely packed within the FTO molecule interspaces [14,17-19]. Further research on the detailed FTO chemical structure needs to be conducted in the future. To further examine the crystallinity and phases of the FTO catalyst, XRD analysis was performed, as shown in Figure 3.

Table 3. Chemical composition of the FTO catalyst using EDX and XPS

Sample	Composition (atomic %) / XPS			Composition (atomic %) / EDX		
	Sn	O	F	Sn	O	F
SnO_2 calcined	32.4	57.9	n.d	24.7	75.3	n.d
FTO calcined	37.6	53.9	1.4	25.0	69.9	5.1

*n.d: not detected

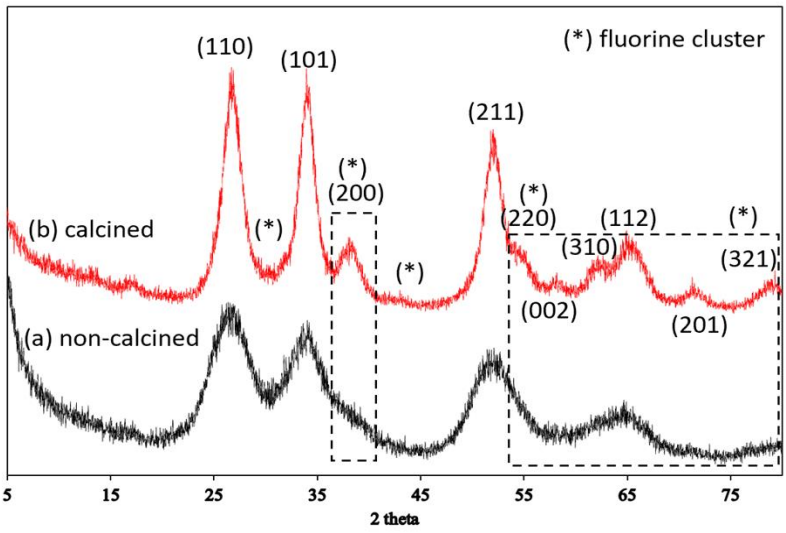

Figure 3. XRD diffractograms overlayed between non-calcined and calcined FTO catalyst

The crystallinity and phases of the FTO catalyst were determined by comparing the XRD patterns for SnO_2 and fluorine phases using JCPDS standards 41-1445 and 74-6155, respectively. The diffraction peaks of the FTO catalyst were seen to have a similar peak to pure SnO_2 and could be indexed as cassiterite with a tetragonal rutile structure [18-21]. These results fit well with the morphology analyses using SEM (Figure 2). The overlayed diffractograms of the non-calcined and calcined FTO catalyst samples show an increase in the crystallinity properties of the FTO catalyst when calcined at high temperature. Some significant peaks were generated in the diffractogram of the calcined FTO catalyst compared with the non-calcined sample. The diffraction peaks with lattices of (200), (220), (002), (310), (201), and (321) were newly formed in the calcined sample. This indicates that the proper crystal structure of the FTO catalyst developed at higher temperatures [22]. The purity of the calcined FTO catalyst increased as the peak intensities increased. The non-calcined FTO diffractogram exhibited an amorphous pattern with broad and insignificant peaks, while the calcined sample showed sharper and more significant peaks. In addition, no specific peaks corresponding to fluorine clusters were detected. The fluorine cluster phases were determined by overlay with SnO_2 main peaks at lattices (200), (220), and (321), indicating good distribution of fluorine clusters in the SnO_2 crystal lattice within the 2θ range of 25 to 35°, and 40 to 45° as well, as due to the emerging fluorine clusters in the FTO molecule [15,23]. The overlaid fluorine clusters were also difficult to detect due to their small size and small amounts of fluorine but EDX and XPS analyses showed a fluorine content in the range of 1.4 to 5.1 wt% respectively [20-21].

Photocatalytic Activity (Optimization of Reaction Parameters)

Influence of Light and Reaction Time on Photocatalytic Activity

In photocatalysis, light wattage and reaction time are crucial parameters that significantly affect catalytic performance. Figure 4 shows the photocatalytic activity of glycerol conversion in 30 min, 60 min and 90 min by light wattage. It was observed that the percentage of glycerol conversion increased with light wattage for 30 min, 60 min and 90 min. The intensity of light radiation affected the rate of photodegradation reaction. Therefore, the higher the light wattage, the higher the percentage of glycerol degradation. The charge carriers, positive holes and electrons resulting from the light irradiation on the FTO catalyst, help produce free radicals, which aid in glycerol degradation [24]. As a result of the increased light, the chances of electron excitation also increased. At higher light wattage, the formation of electron-holes were predominant, whereas the electron-hole recombinant would be negligible. The competition among electron-hole pair separation and recombinants that always occur at low light intensities may reduce the formation of photons to interact with the FTO catalyst [13], thus, decreasing the formation of free radicals, hydroxyl radicals and superoxide ions to undergo redox reaction toward glycerol [25].

In this experiment, the photocatalytic reaction showed an increase in temperature in the range of 29 °C – 39 °C. However, the this was only a small rise in temperature, proving that the glycerol conversion occurred in photocatalysis mode and thus, it was an efficient method due to low energy use.

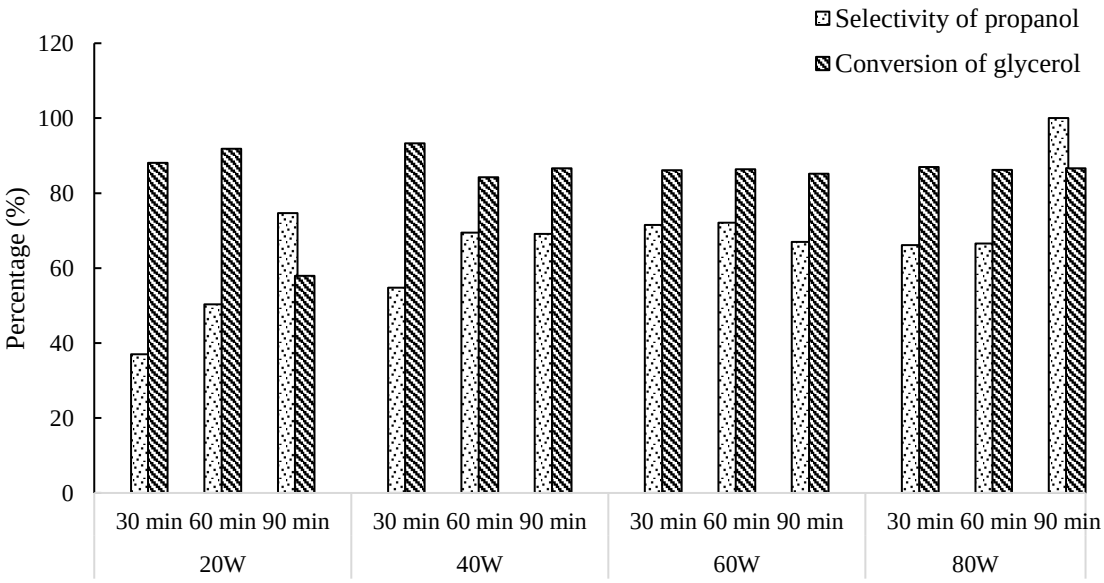

Figure 4. Propanol selectivity and glycerol conversion by light wattage at different reaction times (30 min, 60 min and 90 min)

Based on the result of glycerol conversion and light intensity, the reaction with 40 W in 30 minutes gave the best yield but had a propanol selectivity of only ~54%. Thus, the reaction with 80 W in 90 minutes was chosen as the optimum as it successfully produced 100% propanol selectivity and ~86% glycerol conversion.

Reaction time also has an influence on photodegradation in terms of the adsorption of glycerol onto the photocatalyst surface. Since 80 W of light was chosen as optimal, reaction time was evaluated using only 80 W. Figure 5 shows the photocatalytic activity of propanol based on reaction time using 80 W of light power. From Figure 5, the percentage of glycerol conversion from 30 min to 90 min in 80 W was nearly constant, and relatively stable. The longer the reaction time, the higher the glycerol conversion, as glycerol would have enough time to adsorb and desorb from the photocatalyst. It can be concluded that UV light absorption took at least 30 min to be activated in the photocatalyst.

A study has proved that at low light intensities, the rate of reaction increased linearly with intensity. At intermediate irradiation times beyond a certain value, the rate of reaction would depend on the square root of the light intensity. It is understood that when there are more photons per unit time and unit area, the chances of photon activation on the catalyst surface increase and therefore, photocatalysis can produce free radicals [26]. However, as the light intensity increases, the number of activation sites remains the same. Thus, the reaction rate remains constant even when the light intensity continues to increase [13].

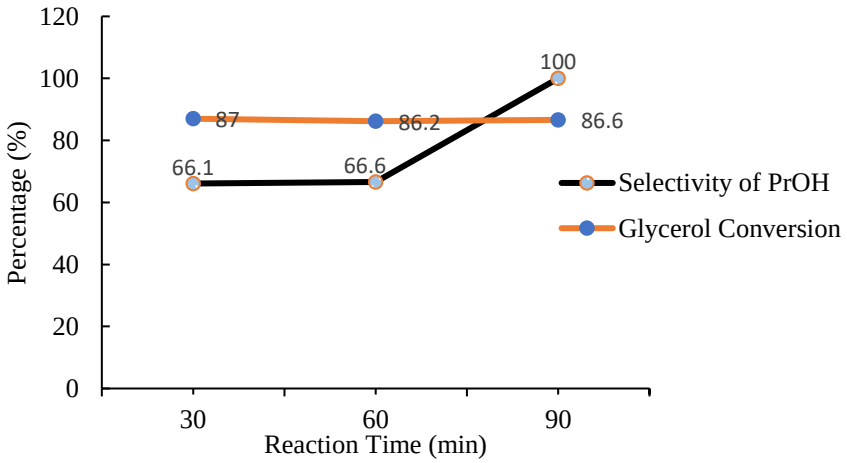

Figure 5. Effects of glycerol conversion and propanol selectivity on reaction time using 80 W of light

That is why glycerol conversion yields may be constant even with increasing reaction time. Furthermore, the selectivity of propanol increased with longer reaction times, showing that there was enough time to complete the reaction even though the conversion yield was unchanged. Hence, 90 minutes at 80 W was the optimum reaction time.

The selectivity (%) of propanol mostly increased with light wattage and reaction time. 100% propanol selectivity was achieved at 80 W in 90 minutes with no by-products formed. Under these conditions, glycerol had sufficient time to be adsorbed on the FTO catalyst. Hence, it had sufficient free radical formation and energy to break the covalent bond of C-O compared to C-C, which was stronger as higher light wattage promotes higher free radical formation [27]. The cleavage of C-O is required to form propanol, while cleavage of C-C would happen when methanol and ethanol are present. Furthermore, both acid and basic sites on the FTO catalyst are thought to promote optimal C-C and C-O bond cleavage. Despite this, the presence of fluoride ions, which act as a Lewis base, was thought to contribute to double dehydration, which performs better under basic conditions [27]. Thus, a basic catalyst can enhance the reduction process, leading to methanol and ethanol production. Figure 6 below shows the proposed mechanism for the reaction of glycerol to propanol as the major product and methanol and ethanol as its side products [5,28-29]. Further studies on the chemical mechanism will be conducted in the future.

With 20 W of UV light, all products had a significant percentage of selectivity. The optimum time for C-C bond breaking was 30 minutes for three carbons to form two carbons resulting in ethanol. A longer reaction time would only cause the C-C bond to break from two carbons to one. That is why ethanol was not detected at 90 minutes. The same trend was observed in 40 W where ethanol was only detected at 30 minutes while for 60 W and 90 W, ethanol was not detected at all. It can be concluded that ethanol only occurs with lower light wattage as the higher the light intensity, the higher the photodegradation, which leads glycerol to favour methanol formation. Propanol took the lead in selectivity from 60 minutes reaction time at 20 W onwards, which showed that the higher the light intensity, the greater the formation of free radicals. Thus, the reaction pathway would promote C-O bond breaking.

It can be concluded that reaction with 80 W in 90 minutes was optimum to produce high selectivity of propanol and high glycerol conversion and yield percentage, respectively (Figure 7). Therefore, this reaction was optimized for another parameter, glycerol concentration.

Influence of Glycerol Concentration on Photocatalytic Activity

There were three different glycerol concentrations analysed, 10 wt%, 15 wt% and 20 wt%, with 1 g of FTO catalyst in 80 W for 90 min. The glycerol conversion slightly decreased from 10 wt% to 15 wt% but increased at 20 wt%. The highest glycerol conversion was 95.5% at 20 wt%. These results are not aligned with many previous studies, where the conversion rate of glycerol was usually reported to be high at low glycerol concentrations [30].

Increased glycerol concentration decreases the photodegradation rate as more glycerol molecules are adsorbed on the FTO surface. Consequently, this reduces the active sites in the FTO catalyst for photons to adsorb and therefore less •OH are formed.

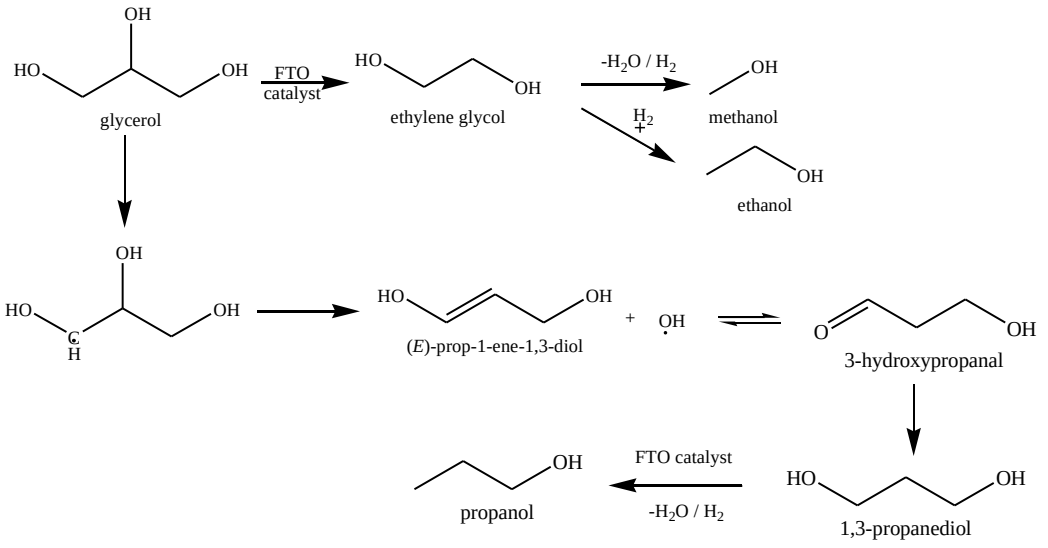

Figure 6. Proposed mechanism for the photocatalysis of glycerol to propanol and other value-added products over FTO [5,28-29]

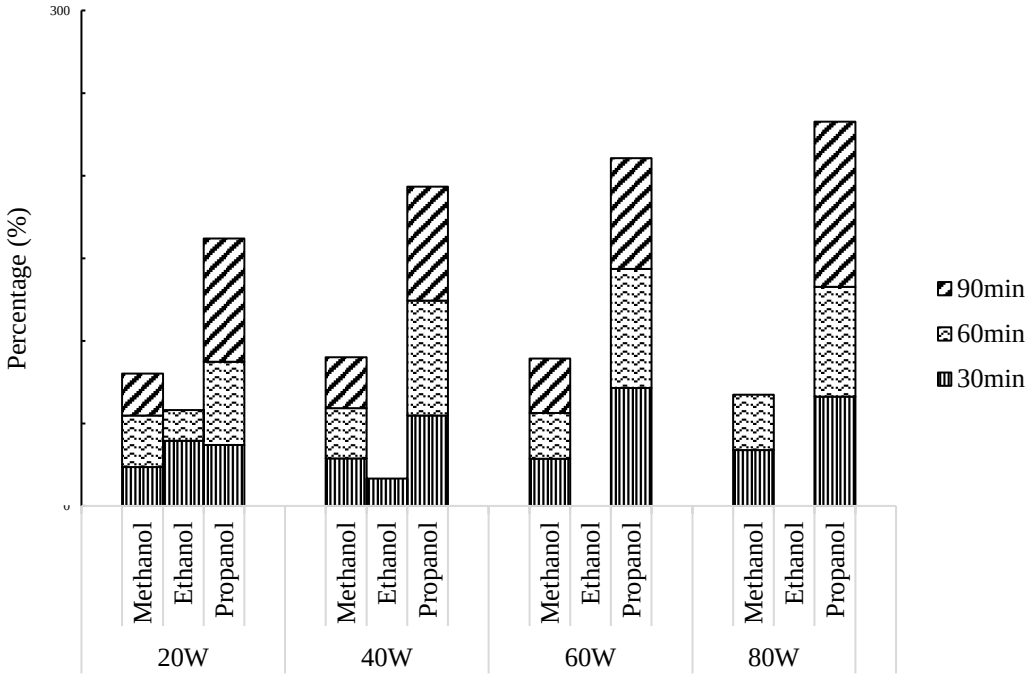

Figure 7. The selectivity of products obtained by photocatalysis based on light wattage and reaction time.

However, in this study, the glycerol conversion was stable ats high percentages in high glycerol concentrations. It is assumed that this condition happened because the basic oxide of the FTO may have undergone thermal dehydration and radical fragmentation which led to higher degradation rates for glycerol [15].

The selectivity and yield of propanol decreased when the glycerol concentration increased. At 15 wt%, isopropanol was detected, although not at 20 wt%. It is possible that the 20 wt% was lacking acid active sites of FTO to convert glycerol to isopropanol and propanol [8]. The selectivity of methanol increased from 15 wt% to 20 wt%, as methanol usually favours basic active sites of FTO [27]. At a lower glycerol concentration (10 wt%), conversion tends to favour products that are easier to form, which only involve C-O bond breaking; therefore, propanol becomes the major product. C-O bond breaking may be due to the cessation of C-C bond dissociation and the onset of the reverse reaction, which selectively cleaves the C-O bond. It could also be due to *in situ* catalyst oxidation, which increases methanol production to an optimal level, causing glycerol to be transformed to propanol [31]. At higher glycerol concentrations, the FTO catalyst was more active in breaking the C-C bond, which usually requires higher temperatures. Hence, it can be concluded that the products obtained were various due to the flexible characteristics of FTO, which depend on the reaction parameters. Figure 8 presents the glycerol conversion and product selectivities based on different glycerol concentrations. Compared to FTO photocatalytic activity, a standard SnO_2 sample was conducted under optimum reaction parameters (80 W, 90 minutes, 10 wt% glycerol concentration). The glycerol conversion and propanol selectivity were recorded at 46 % and 54.7%, respectively. The results show that fluorine doping of the SnO_2 molecule could generate a fluoride ion (F^-) that substitutes for the oxygen (O^{2-}) vacancies, thus contributing to at least one extra electron [20]. Addition of electrons could assist the reduction/dehydration process in the conversion of glycerol to propanol.

CONCLUSION

In conclusion, the photocatalytic conversion of glycerol to propanol using an FTO catalyst was successfully studied. The optimal reaction time and light wattage were determined to be 90 minutes and 80 W, respectively, using 1 g of FTO and 10 wt% glycerol concentration. Under these conditions, a high glycerol conversion of 86 % and propanol selectivity of 100% were observed. The FTO catalyst was very dynamic as various products could be formed by changing reaction parameters. As proven in this research, when different glycerol concentrations were used, other products such as methanol increased in terms of selectivity. Therefore, the amphoteric and conducting properties of the FTO catalyst provide a new platform for effective biomass (glycerol) degradation into value-added chemicals such as propanol, methanol, and ethanol. In the future, optimization of parameters such as catalyst weight and calcination temperature, as well as improving the FTO catalyst with a metal support, may assist in a better

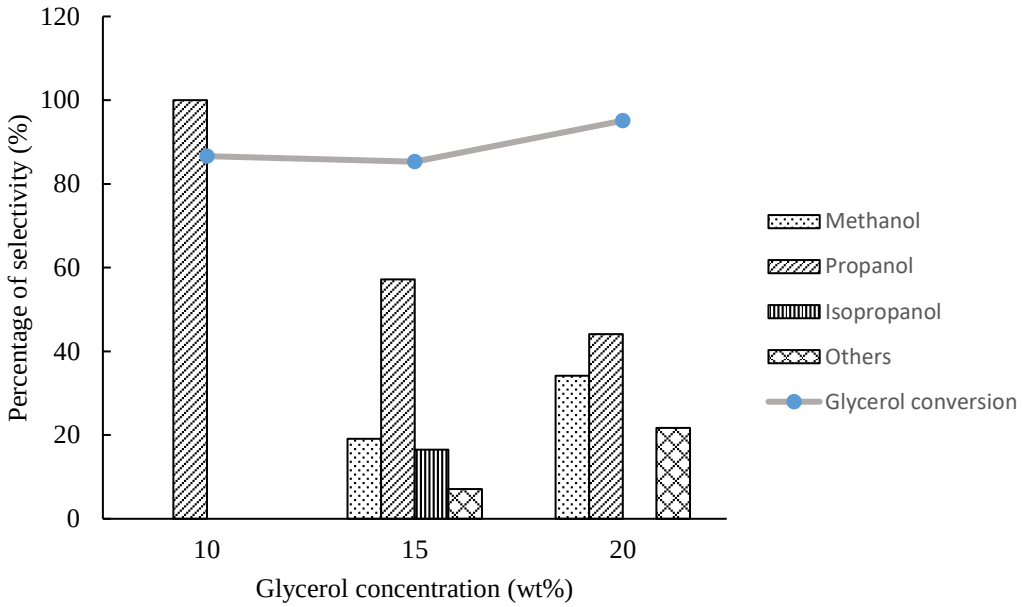

Figure 8. The catalytic activity results obtained with different glycerol concentrations

understanding of the photocatalytic activity of FTO. Photocatalysis is also an environmentally-friendly method as it requires little energy and ambient temperatures.

ACKNOWLEDGEMENTS

The authors would like to acknowledge funding from the Ministry of Higher Education of Malaysia, with grant number 600-ITMI/FRGS 5/3 (403/2019).

The authors declare that they have no conflict of interest.

REFERENCE

1. Bagnato, G., Iulianelli, A., Sanna, A., and Basile, A. (2017) Glycerol production and transformation: A critical review with particular emphasis on glycerol reforming reaction for producing hydrogen in conventional and membrane reactors. *Membranes*, **7(2)**, 1–31.

2. He, Q., Mcnutt, J. and Yang, J. (2017) Utilization of the residual glycerol from biodiesel production for renewable energy generation. *Renewable and Sustainable Energy Reviews*, **71**, 63–76.

3. Fan, X., Burton, R. and Zhou, Y. (2010) Glycerol (Byproduct of Biodiesel Production) as a source for fuels and chemicals – Mini Review. *The Open Fuels & Energy Science Journal*, **3(1)**, 17–22.

4. Kostyniuk, A., Bajec, D. and Likozar, B. (2020) One step synthesis of ethanol from glycerol in a gas phase packed bed reactor over hierarchical alkali-treated zeolite catalyst materials. *Green Chemistry*, **22**, 753-765.

5. Miyazawa, T., Kusunoki, Y., Kunimori, K. and Tomishige, K. (2006) Glycerol conversion in the aqueous solution under hydrogen over Ru/C an ion- exchange resin and its reaction mechanism. *Journal of Catalysis*, **240(2)**, 213– 221.

6. Yu, L., Yuan, J., Zhang, Q., Liu, Y. -M., He, H. -Y., Fan, K. -N. and Cao, Y. (2014) Propylene from renewable resources: catalytic conversion of glycerol into propylene. *ChemSusChem*, **7(3)**, 743–747.

7. Zhou, C. -H. C., Beltramini, J. N., Fan, Y. -X. and Lu, G. Q. (2008) Chemoselective catalytic conversion of glycerol as a biorenewable source to valuable commodity chemicals. *Chem. Soc. Rev.*, **37(3)**, 527–549.

8. Gatti, M. N., Cerioni, J. L., Pompeo, F., Santori, G. F. and Nichio, N. N. (2020) High yield to 1-propanol from crude glycerol using two reaction steps with Ni catalysts. *Catalysts*, **10(6)**, 615.

9. Payormhorm, J. and Idem, R. (2020) Synthesis of C-doped TiO2 by sol-microwave method for photocatalytic conversion of glycerol to value-added chemicals under visible light. *Applied Catalysis A: General*, **590**, 117362.

10. Granone, L. I., Sieland, F., Zheng, N., Dillert, R. and Bahnemann, D. W. (2018) Photocatalytic conversion of biomass into valuable products: A meaningful approach? *Green Chemistry*, **20(6)**, 1169–1192.

11. Nakata, K. and Fujishima, A. (2012) TiO2 photocatalysis: Design and applications. *Journal of Photochemistry and Photobiology C: Photochemistry Reviews*, **13(3)**, 169–189.

12. Stelmachowski, M., Marchwicka, M., Grabowska, E., Diak, M. and Zaleska, A. (2014) The photocatalytic conversion of (Biodiesel Derived) glycerol to hydrogen - A short review and preliminary experimental results Part 2: photocatalytic conversion of glycerol to hydrogen in batch and semi-batch laboratory reactors. *Journal of Advanced Oxidation Technologies*, **17(2)**, 179–186.

13. Limpachanangkul, P., Liu, L., Hunsom, M. and Chalermsinsuwan, B. (2020) Low energy photocatalytic glycerol conversion to high valuable products via Bi2O3 polymorphs in the presence of H2O2. *Energy Reports*, **6**, 95–101.

14. Samad, W. Z., Isahak, W. N., Liew, K. H., Nordin, N., Yarmo, M. A. and Yusop, M. R. (2014) Ru/FTO: Heterogeneous catalyst for glycerol hydrogenolysis. *AIP Conference Proceeding*, **1614(1)**, 269.

15. Haddad, N., Ben Ayadi, Z., Mahdhi, H. and Djessas, K. (2017) Influence of fluorine doping on the microstructure, optical and electrical properties of SnO2 nanoparticles. *Journal of Materials Science: Materials in Electronics*, **28(20)**, 15457–15465.

16. Thakur, P. and Joshi, S. S. (2012) Effect of alcohol and alcohol/water mixtures on crystalline structure of CdS nanoparticles. *Journal of Experimental Nanoscience*, **7(5)**, 547–558.

17. Samad, W. Z., Salleh, M. M., Shafiee, A. and Yarmo, M. A. (2011) Structural, optical and electrical properties of fluorine doped tin oxide thin films deposited using inkjet printing technique. *Sains Malaysiana*, **40(3)**, 251–257.

18. Samad, W. Z., Goto, M., Kanda, H., Wahyudiono, Nordin, N., Liew, K. H. and Yusop, M. R. (2017) Fluorine-doped tin oxide catalyst for glycerol conversion to methanol in sub-critical water. *The Journal of Supercritical Fluids*, **120**, 366-378.

19. Martinez, A. I., Huerta, L., De Leon, J. M. O. R., Acosta, D., Malik, O. and Aguilar, M. (2006) Physicochemical characteristics of fluorine doped tin oxide films. *J. Phys. D Apply. Phys.*, **39**, 5091–5096.

20. Wang, X., Wang, X., Di, Q., Zhao, H. and Yang, J. (2017) Mutual effects of fluorine dopant and oxygen vacancies on structural and luminescence characteristics of F doped SnO_2 nanoparticles. *Materials*, **10(12)**, 1398.

21. Liu, H., Wang, A., Sun, Q., Wang, T. and Zeng, H. (2017) Cu nanoparticles/fluorine-doped tin oxide (FTO) nanocomposites for photocatalytic H2 evolution under visible light irradiation. *Catalysts*, **7**, 385.

22. Zhu, S., Gao, X., Zhu, Y., Fan, W., Wang, J. and Li, Y. (2015) A highly efficient and robust Cu/SiO2 catalyst prepared by the ammonia evaporation hydrothermal method for glycerol hydrogenolysis to 1,2-propanediol. *Catalysis Science & Technology*, **5**, 1169–1179.

23. Ma, L., He, D. and Li, Z. (2008) Promoting effect of rhenium on catalytic performance of Ru catalyst in hydrogenolysis of glycerol to propanediol. *Catal. Commun*, **9**, 2489–2495.

24. Gusain, R., Kumar, N. and Ray, S. S. (2020) Factors influencing the photocatalytic activity of photocatalysts in wastewater treatment. *Photocatalysts in Advanced Oxidation Processes for Wastewater Treatment*, **8**, 229–270.

25. Neppolian, B. (2002) Solar/UV-induced photocatalytic degradation of three commercial textile dyes. *Journal of Hazardous Materials*, **89(2-3)**, 303–317.

26. Reza, K. M., Kurny, A. S. W. and Gulshan, F. (2015) Parameters affecting the photocatalytic degradation of dyes using TiO2: a review. *Applied Water Science*, **7(4)**, 1569–1578.

27. Haider, M. H., Dummer, N. F., Knight, D. W., Jenkins, R. L., Howard, M., Moulijn, J., Taylor, S. H. and Hutchings, G. J. (2015) Efficient Green methanol synthesis from glycerol. *Nature Chemistry*, **7(12)**, 1028–1032.

28. Fujishima, A., Zhang, X. and Tryk, D. (2008) TiO2 photocatalysis and related surface phenomena. *Surface Science Reports*, **63(12)**, 515–582.

29. Cheng, L., Liu, L. and Ye, X. P. (2012) Acrolein Production from Crude Glycerol in Sub- and Super-Critical Water. *Journal of the American Oil Chemists' Society*, **90(4)**, 601–610.

30. Bienholz, A., Schwab, F. and Claus, P. (2010) Hydrogenolysis of glycerol over a highly active CuO/ZnO catalyst prepared by an oxalate gel method: influence of solvent and reaction temperature on catalyst deactivation. *Green Chem.*, **12(2)**, 290– 295.

31. Xi, Z., Hong, Z., Huang, F., Zhu, Z., Jia, W. and Li, J. (2020) Hydrogenolysis of glycerol on the ZRO2-TiO2 supported PT-Wox Catalyst. *Catalysts*, **10(3)**, 312.